

Ferromagnetic imprinting of spin polarization in a semiconductor

C. Ciuti, J. P. McGuire, and L. J. Sham

Department of Physics, University of California San Diego, La Jolla CA 92093-0319.

(Dated: November 13, 2018)

We present a theory of the imprinting of the electron spin coherence and population in an n-doped semiconductor which forms a junction with a ferromagnet. The reflection of non-equilibrium semiconductor electrons at the interface provides a mechanism to manipulate the spin polarization vector. In the case of unpolarized excitation, this ballistic effect produces spontaneous electron spin coherence and nuclear polarization in the semiconductor, as recently observed by time-resolved Faraday rotation experiments. We investigate the dependence of the spin reflection on the Schottky barrier height and the doping concentration in the semiconductor and suggest control mechanisms for possible device applications.

The physics of the semiconductor/ferromagnet interface is a crucial issue in the emerging field of spin electronics [1]. Progress has been made in injecting polarized electrons from ferromagnets [2, 3, 4, 5] or semimagnetic semiconductors [6, 7, 8, 9] into semiconductors, an essential step towards the exploitation of the spin degree of freedom in a new generation of multifunctional devices. Recently, time-resolved optical Faraday rotation measurements have demonstrated that the presence of a ferromagnetic interface [10, 11] can produce spontaneous electron spin coherence and large nuclear magnetic fields in the semiconductor. Moreover, the spin-polarized photocurrent from a semiconductor into a ferromagnet [12, 13] has been shown to vary with optical polarization. We report here a theoretical study of the spin reflection of non-equilibrium electrons at the semiconductor/ferromagnet interface. Our results show how (1) unpolarized electrons *in the semiconductor* are spontaneously polarized and (2) a pre-existing spin polarization vector is tilted. The underlying physics is reminiscent of the Mott scattering [14] of electrons with atoms via spin-dependent interaction.

Our theory is based on the general scattering theory of the electron spin density matrix [14]. In particular, we focus on tunneling through an insulator layer [15, 16] or a Schottky barrier [17]. The source of the electrons may be electrical or optical. The non-equilibrium carriers produce a spin current into the ferromagnet during the short momentum relaxation time following a pulsed excitation. This ultrafast ballistic process leaves a net spin coherence and population in the semiconductor. We show how to extract from the time-resolved Faraday rotation the ballistic spin transport properties of the semiconductor/ferromagnetic junction and predict the dependence of the imprinted spin on the system parameters.

The Hamiltonian for the semiconductor/ferromagnet junction (see Fig. 1a-b),

$$H = K + V(x) + \frac{g^*}{2} \mu_B \boldsymbol{\sigma} \cdot \mathbf{B}_T \Theta(-x) + \frac{\Delta}{2} \sigma_M \Theta(x), \quad (1)$$

consists of: the kinetic energy K for the conduction band on the semiconductor side and two spin bands

with exchange splitting Δ in the ferromagnet; the Schottky barrier potential $V(x)$; the Zeeman energy in the semiconductor where g^* is the effective electron g-factor ($g_{\text{GaAs}}^* = -0.44$), μ_B the Bohr magneton, and $\boldsymbol{\sigma}$ the vector of Pauli matrices. The total field \mathbf{B}_T is the sum of the applied field \mathbf{B} and of the local field \mathbf{B}_N due to the nuclear polarization. σ_M is the Pauli matrix in the magnetization direction and Θ is the step function. The orbital effect of the weak magnetic field is neglected.

The contribution to the spin polarization by the valence holes can be neglected since the hole spin relaxation time is much shorter than the optical recombination time T_{rec} [18] due to spin mixing in the valence bands by the spin-orbit interaction[19]. The spin dephasing time of the conduction electron in n-doped samples is shown to be much longer than the recombination time [20]. Because of the dominant role of the magnetization in the ferromagnet, we denote the majority and minority spin states by $|+\rangle$ and $|-\rangle$ respectively. These states are eigenstates of the ferromagnetic exchange splitting operator, namely $\sigma_M |\pm\rangle = \mp |\pm\rangle$ (note that the magnetization \mathbf{M} is antiparallel to the net electron spin \mathbf{S}^{fm}). The spin-dependent reflection of the semiconductor electrons at the ferromagnetic interface is represented by the reflection matrix $\hat{r}(\mathbf{k})$ in the electron spin space. In the ferromagnetic spin basis $\{|-\rangle, |+\rangle\}$, the reflection matrix has the diagonal representation $\hat{r}(\mathbf{k}) = |-\rangle r_{-, \mathbf{k}} \langle -| + |+\rangle r_{+, \mathbf{k}} \langle +|$, where $r_{-, \mathbf{k}}$ ($r_{+, \mathbf{k}}$) is the reflection coefficient for a semiconductor electron spin aligned with the ferromagnet minority (majority) spin band. This diagonal representation in the ferromagnetic spin basis is exact only if the semiconductor magnetic field \mathbf{B}_T is parallel to the magnetization \mathbf{M} . However, the exchange splitting Δ in a ferromagnet is typically several orders of magnitude larger than the semiconductor Zeeman splitting. We have verified explicitly that the effect of the magnetic field \mathbf{B}_T on the spin-dependent reflection matrix is negligible. Also, the effective magnetic field due to the lack of the inversion symmetry (the Rashba effect) is negligible here. For extraction of the spin polarization, it is convenient to ex-

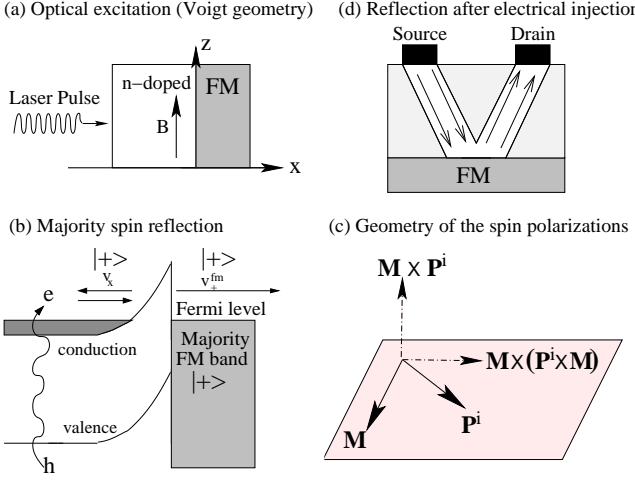


FIG. 1: Counterclockwise: (a) Sketch of the semiconductor/ferromagnet junction excited by a light beam in Voigt configuration. (b) Schematic band diagram for the reflection and transmission of a semiconductor electron in the majority spin channel ($|+\rangle$) is the spin state of the ferromagnetic majority band). For the minority spin band the diagram is analogous, but with a different Fermi velocity. (c) Geometry involved in the ferromagnetic imprinting when the pumped electrons have a spin polarization \mathbf{P}^i . The polarization of the reflected electrons will have also a component along $\hat{\mathbf{M}} \times \mathbf{P}^i$, i.e. orthogonal to the ferromagnet magnetization and the incident polarization (see Eq. (7)). When $\mathbf{P}^i = 0$, the imprinted spin is directed along $\hat{\mathbf{M}}$. (d) Sketch of electrical device where ballistic electrons are injected through lateral contacts.

press the reflection matrix in the form

$$\hat{r}(\mathbf{k}) = \frac{1}{2} \left[(r_{-,k} + r_{+,k}) \mathbb{1} + (r_{-,k} - r_{+,k}) \hat{\mathbf{M}} \cdot \boldsymbol{\sigma} \right], \quad (2)$$

where $\mathbb{1}$ is the unit matrix and $\hat{\mathbf{M}}$ is the unit vector along the magnetization.

Consider the excitation of the n-doped semiconductor by a short optical pulse. Immediately after the light absorption, the excited electron spin density matrix on the semiconductor side is $\hat{\rho}^i(\mathbf{k}, t=0) = f^i(k) \frac{1}{2} (\mathbb{1} + \mathbf{P}^i \cdot \boldsymbol{\sigma})$, where $f^i(k)$ is the non-equilibrium electron distribution injected by the exciting laser. The polarization vector \mathbf{P}^i depends on the optical selection rules. Since the pump has injected electrons, there will be an electron current (per unit area) from the semiconductor into the ferromagnet,

$$\hat{j}(t) = \hat{j}^i(t) + \hat{j}^r(t) = \int_{k_x > 0} \frac{d^3 \mathbf{k}}{(2\pi)^3} [\hat{\rho}^i(\mathbf{k}, t) - \hat{\rho}^r(\mathbf{k}, t)] v_x, \quad (3)$$

where $v_x = \hbar k_x / m_s$ is the velocity component normal to the interface. The reflected density matrix is given by

$$\hat{\rho}^r(\mathbf{k}, t) = \hat{r}(\mathbf{k}) \hat{\rho}^i(\mathbf{k}, t) \hat{r}^\dagger(\mathbf{k}) \quad (4)$$

$$= f^i(k, t) \frac{1}{2} [R_0(\mathbf{k}) \mathbb{1} + \mathbf{R}(\mathbf{k}) \cdot \boldsymbol{\sigma}], \quad (5)$$

where, with the \mathbf{k} -dependence understood,

$$R_0 = \frac{1}{2} [(|r_-|^2 + |r_+|^2) + (|r_-|^2 - |r_+|^2) \hat{\mathbf{M}} \cdot \mathbf{P}^i], \quad (6)$$

$$\begin{aligned} \mathbf{R} = & \frac{1}{2} [(|r_-|^2 - |r_+|^2) + (|r_-|^2 + |r_+|^2) \hat{\mathbf{M}} \cdot \mathbf{P}^i] \hat{\mathbf{M}} \\ & + \text{Re}(r_- r_+^*) (\hat{\mathbf{M}} \times \mathbf{P}^i) \times \hat{\mathbf{M}} - \text{Im}(r_- r_+^*) \hat{\mathbf{M}} \times \mathbf{P}^i. \end{aligned} \quad (7)$$

The time-dependence of $\hat{\rho}^i(\mathbf{k}, t)$ is dominated by the relaxation of the hot carrier distribution $f^i(k, t)$. The spin precession due to a weak applied magnetic field and spin relaxation occur on a much longer time scale compared to the fast orbital relaxation. In the relaxation time approximation, the decay of the non-equilibrium electron population is $f^i(k, t) = f^i(k) \exp(-t/\tau_k)$, yielding a simple expression for the surface spin density imprinted in the semiconductor,

$$\begin{aligned} \mathbf{S}^r &= -\text{Tr} \left\{ \frac{\hbar}{2} \boldsymbol{\sigma} \int dt [\hat{j}^i(t) + \hat{j}^r(t)] \right\} \\ &= \frac{\hbar}{2} \int_{k_x > 0} \frac{d^3 \mathbf{k}}{(2\pi)^3} f^i(k) [\mathbf{R}(\mathbf{k}) - \mathbf{P}^i] \tau_k v_x. \end{aligned} \quad (8)$$

After the transient, the surface spin density inherited by the n-doped semiconductor is $\mathbf{S}^{\text{tot}} = n^i L \frac{\hbar}{2} \mathbf{P}^i + \mathbf{S}^r$ where $n^i = \int \frac{d^3 \mathbf{k}}{(2\pi)^3} f^i(k)$ is the volume density of pumped electrons and L is the sample length. Of course, this holds when n^i is smaller than the doping density n (acting as a spin reservoir) and when L is larger than the mean-free path. In fact, for very thin samples, our treatment needs to be refined to account for multiple reflections.

In the following, we will consider separately the two cases of spin unpolarized and polarized excitation.

(i) Unpolarized excitation

The injected electron ensemble is unpolarized ($\mathbf{P}^i = 0$). Reflection from the ferromagnet results in a net spin surface density,

$$\mathbf{S}^r = \frac{\hbar}{4} \hat{\mathbf{M}} \int_{k_x > 0} \frac{d^3 \mathbf{k}}{(2\pi)^3} f^i(k) (|r_{-,k}|^2 - |r_{+,k}|^2) \tau_k v_x. \quad (9)$$

The amplitude of the imprinted spin in the semiconductor is determined by the difference between the spin-dependent reflectivities. For each momentum channel the mean free path is $\tau_k v_x$. Finally, \mathbf{S}^r is aligned either parallel or antiparallel to the ferromagnetic magnetization \mathbf{M} , depending on the interface properties, which will be shown below.

In an applied magnetic field \mathbf{B} , the Larmor precession of the imprinted spin polarization is given by $\partial_t \mathbf{S}(t) = \frac{1}{\hbar} g^* \mu_B \mathbf{B}_T \times \mathbf{S}(t) - \frac{1}{T_2} \mathbf{S}(t)$, where T_2 is the spin relaxation time and the initial condition is $\mathbf{S}(t \approx 0) = \mathbf{S}^r$. The total field $\mathbf{B}_T = \mathbf{B} + \mathbf{B}_N$ contains the local contribution \mathbf{B}_N due to the nuclear polarization [21] where

$\mathbf{B}_N \sim (g^*/|g^*|)(\mathbf{S}^r \cdot \mathbf{B}) \mathbf{B}/B^2$. The imprinting of the nuclear spins also affects the effective Larmor precession frequency $\Omega_L = g^*\mu_B(B + B_N)/\hbar$ [22] which can be measured by the time-resolved optical Faraday rotation [10, 11]. The Faraday rotation of a linearly polarized probe beam is proportional to the component of the net electron spin along the direction of the photon wave-vector \mathbf{k}_{phot} in the medium, i.e. $\text{FR}(t) \sim \mathbf{S}(t) \cdot \mathbf{k}_{\text{phot}}/k_{\text{phot}}$. Now, consider the Voigt geometry with light propagating along the x direction and magnetic field in the z direction. Let the ferromagnetic magnetization be in the interface plane at an angle α to \mathbf{B} (i.e. $\mathbf{M} = M(0, \sin \alpha, \cos \alpha)$). Since $g^* < 0$, the nuclear field is $B_N \sim \langle (|r_+|^2 - |r_-|^2) \tau v_x \rangle \cos \alpha$. The spontaneous Faraday rotation is $\text{FR}(t) \sim \langle (|r_-|^2 - |r_+|^2) \tau v_x \rangle \sin \alpha \sin(\Omega_L t) e^{-t/T_2}$. Therefore, for $\alpha = 0$ the nuclear imprinting is maximum while there is no spontaneous Faraday rotation. On the other hand, for $\alpha = \pi/2$, the nuclear field vanishes while the spontaneous coherence has the maximum amplitude. Moreover, the Faraday rotation oscillates in time as $\sin(\Omega_L t)$. These trends are in perfect agreement with the experimental observations [10, 11]. The theory predicts similar spin polarization effects when an unpolarized current is injected electrically, for example through a ballistic V-groove with non-magnetic contacts as shown in Fig. 1d.

(ii) Polarized excitation

When the excited electron population has a pre-existing spin polarization ($\mathbf{P}^i \neq \mathbf{0}$), the current in the semiconductor is changed by the spin polarization and the spin polarization is altered. In addition to two components in the plane defined by the magnetization and initial polarization vectors, there will be an additional component normal to the plane [cf. Eq. (7)], as shown in Fig. 1c. Evidence for polarization-dependence of the ferromagnetic imprinting has been reported in Ref. 11. Additional studies as a function of the relative orientation between $\hat{\mathbf{M}}$ and \mathbf{P}^i will be needed to test the dependence predicted in Eq. (7). Such a change of the spin polarization direction could provide a mechanism for the manipulation of the semiconductor spin polarization vector.

For the phenomena discussed above to be measurable, the spin-dependence of the reflection coefficients need to be sufficiently strong. We point out that since the transmittance $|t|^2 = 1 - |r|^2$ in either direction through the barrier is the same, reflection in the semiconductor is no more efficient in creating spin polarization than injection from the ferromagnet. To investigate the dependence on the parameters of the Schottky barrier, we calculate the spin-dependent reflection coefficients for a simplified model of the semiconductor/ferromagnet junction. We consider first a rectangular barrier $V(x < 0) = U_b \Theta(x + a) - E_s \Theta(-x - a)$, where U_b is the barrier height measured from the Fermi level and $E_s = \hbar^2(3\pi^2n)^{2/3}/(2m_s)$ is the kinetic Fermi energy of the n-doped semiconductor. The spin-dependent reflec-

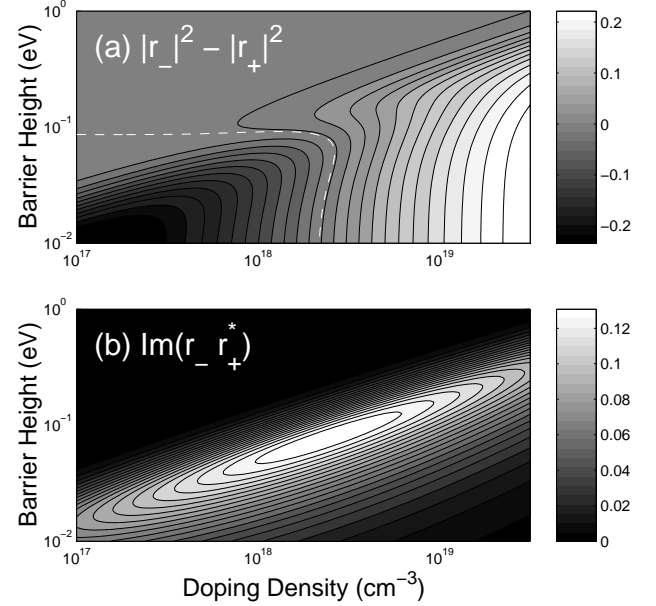


FIG. 2: (a) Contours of $|r_{-,k}|^2 - |r_{+,k}|^2$ as a function of the doping density n (log scale) and the Schottky barrier height U_b (log scale). For each density, \mathbf{k} is taken along the x -direction with amplitude $(3\pi^2n)^{1/3}$, the Fermi wavevector in the n-semiconductor. The semiconductor parameters are those of bulk GaAs. Ferromagnet Fermi velocities: $v_+^{\text{fm}} = 9.4 \times 10^7 \text{ cm/s}$, $v_-^{\text{fm}} = 4.6 \times 10^7 \text{ cm/s}$ (corresponding to two exchange split parabolic bands with $E_F = 2.5 \text{ eV}$, $\Delta = 1.9 \text{ eV}$ and free-electron mass). At the white-dashed line, $|r_{-,k}|^2 - |r_{+,k}|^2$ changes sign. (b) Contours of $\text{Im}(r_- r_+^*)$. $\text{Im}(r_- r_+^*)$ has always the same sign.

tion coefficients are

$$r_{\pm, \mathbf{k}} = \frac{e^{2k_b a} (iv_{\pm}^{\text{fm}} - v_b)(iv_x + v_b) - (iv_{\pm}^{\text{fm}} + v_b)(iv_x - v_b)}{e^{2k_b a} (iv_{\pm}^{\text{fm}} - v_b)(iv_x - v_b) - (iv_{\pm}^{\text{fm}} + v_b)(iv_x + v_b)},$$

where v_{\pm}^{fm} is the Fermi velocity (along the x -direction) of the majority (minority) band in the ferromagnet. In the simplified case of two parabolic bands, $v_+^{\text{fm}} = \sqrt{2E_F/m_{\text{fm}}}$ and $v_-^{\text{fm}} = \sqrt{2(E_F - \Delta)/m_{\text{fm}}}$, implying that $v_+^{\text{fm}} > v_-^{\text{fm}}$. Note that a non-parabolic band dispersion can lead to an opposite relationship, i.e. $v_+^{\text{fm}} < v_-^{\text{fm}}$. The wave-vector $k_b = \sqrt{2m_s(U_b + E_s)/\hbar^2 - k_x^2}$ is that of the evanescent wave in the barrier region and $v_b = \hbar k_b/m_s$. Finally, $v_x = \hbar k_x/m_s$ is the incident velocity in the semiconductor. A more realistic Schottky barrier is represented by a parabolic bent potential $V(x)$ (see Fig. 1b) with depletion layer $d \approx \sqrt{\epsilon_0 U_b / (2\pi n e^2)}$ where ϵ_0 the dielectric constant. To improve our estimate, for each value of k_x we approximate the reflection coefficients by taking an effective rectangular barrier width $a = a(k_x)$ such that the action integral in the barrier region is the same.

Representative results for realistic material parameters are plotted in Fig. 2. Panel (a) shows contours of $|r_{-,k}|^2 - |r_{+,k}|^2$ as a function of the doping density n

and the barrier height U_b . In the region where tunneling is significant, the predicted difference between majority and minority reflectivities can be 25 % (the polarization is actually large also when tunneling is small [23]). When $|r_{-,k}|^2 - |r_{+,k}|^2$ is positive (negative), the imprinted spin \mathbf{S}^r is parallel (antiparallel) to the magnetization \mathbf{M} in the ferromagnet. For vanishing barrier height and low doping, the transmittance into the ferromagnet is dominated by the spin channel with the lower ferromagnet Fermi velocity, allowing a better matching with the small semiconductor velocity. However, with increasing doping, the semiconductor velocity increases and eventually can match better the ferromagnet spin band with the larger velocity. This is the reason for the change of sign of $|r_{-,k}|^2 - |r_{+,k}|^2$ as a function of doping in the low barrier region. When the barrier height is large enough, the velocity matching is not the only relevant feature. Indeed, for moderate doping a barrier increase can induce a change of sign of $|r_{-,k}|^2 - |r_{+,k}|^2$ in analogous way to what is predicted for ferromagnet/oxide junctions [15]. This prediction suggests that by using a forward bias (i.e., semiconductor Fermi level higher than that in the metal) to tune the semiconductor barrier U_b , the sign and amplitude of the imprinted spin could be controlled.

Actually, different spin orientations with different materials have been observed experimentally [11]. In a GaAs/MnAs heterojunction, \mathbf{S}^r has been found to be antiparallel to \mathbf{M} , while for a GaAs/Fe system the spin is parallel. Recent transport characterizations of GaAs/MnAs suggest that the Schottky barrier in this system can be very low, allowing nearly ohmic conduction [24] and significant spin valve effect in trilayer structures [25]. In the case of iron, the barrier is quite high (0.7 eV) and thus our model predicts an imprinted spin parallel to \mathbf{M} as observed [11]. The relatively high efficiency observed in the case of the iron junction at very low doping density ($\approx 10^{17} \text{ cm}^{-3}$) [11] may be due to the very thin GaAs active region ($L = 100 \text{ nm}$) of the investigated sample. The effects of finite size on the Schottky barrier and of multiple electron reflections could significantly enhance the spin reflection efficiency, an issue under current investigation. To complete our study, Fig. 2b depicts the contours of $\text{Im}(r_- r_+^*)$, representing the amplitude of the component of the imprinted spin along $\hat{\mathbf{M}} \times \mathbf{P}^i$ (see Eq. (7)) which we predict to occur when the excited electrons are already polarized ($\mathbf{P}^i \neq \mathbf{0}$).

In conclusion, we have presented a ballistic theory for the ferromagnetic imprinting of the spin coherence and population in an n-doped semiconductor following pulsed excitation. We have given an analysis of the optical pumping and the all-optical detection of spin transport through the time-resolved Faraday rotation, giving a framework for the interpretation of recent experiments [10, 11]. We suggest that an electrical tuning of the Schottky barrier could allow for control of the sign and

amplitude of the imprinted spin. For the possibilities of device applications, generation of spin currents and re-orientation of the spin polarization are predicted also for electrical excitation of non-equilibrium electrons in the semiconductor using traditional non-magnetic contacts. Detailed studies of particular systems and quantitative comparison with experiments will be given elsewhere.

This work is supported by DARPA/ONR N0014-99-1-1096 and NSF DMR 0099572. CC is also grateful to the Swiss National Foundation for additional support. JPM acknowledges a graduate fellowship by California Institute for Telecommunications and Information Technology. We thank D.D. Awschalom for discussions and for the experimental results [11] prior to publication.

- [1] S.A. Wolf *et al.*, *Science* **294**, 1488 (2001).
- [2] Y. Ohno, *et al.*, *Nature* **402**, 790 (1999).
- [3] P.R. Hammer, B.R. Bennett, M.J. Yang, and M. Johnson, *Phys. Rev. Lett.* **83**, 203 (1999) and **84**, 5024 (2000). F.G. Monzon, H.X. Tang, and M.L. Roukes, *ibid* **84**, 5022 (2000). B.J. van Wees, *ibid* **84**, 5023 (2000).
- [4] H.J. Zhu, *et al.*, *Phys. Rev. Lett.* **87**, 016601 (2001).
- [5] A.T. Hanbicki, *et al.*, *Appl. Phys. Lett.* **80**, 1240 (2002).
- [6] B.T. Jonker, U.S. Patent No. 5,874,749 (filed in 1993, awarded in 1999). B.T. Jonker, *et al.*, *Phys. Rev. B* **62**, 8180 (2000).
- [7] R. Fiederling, *et al.*, *Nature* **402**, 787 (1999).
- [8] I. Malajovich, *et al.*, *Nature* **411**, 770 (2001).
- [9] M. Ghali, *et al.*, *Solid State Commun.* **119**, 371 (2001).
- [10] R.K. Kawakami *et al.*, *Science* **294**, 131 (2001).
- [11] R.J. Epstein *et al.*, to be published in *Phys. Rev. B*; preprint cond-mat/0201350.
- [12] A. Hironata *et al.*, *Phys. Rev. B* **63**, 104425 (2001).
- [13] A.F. Isakovic, *et al.*, *Phys. Rev. B* **64**, 161304 (2001).
- [14] N.F. Mott and H.S.W. Massey, *The theory of atomic collisions*, third edition (Oxford University Press, London, 1965), Chapter X.
- [15] J.C. Slonczewski, *Phys. Rev. B* **39**, 6995 (1989).
- [16] R. Jansen, M.W.J. Prins, and H. Van Kempen, *Phys. Rev. B* **57**, 4033 (1998).
- [17] E.I. Rashba, *Phys. Rev. B* **62**, R16267 (2000).
- [18] T.C. Damen *et al.*, *Phys. Rev. Lett.* **67**, 3432 (1991).
- [19] T. Uenoyama and L.J. Sham, *Phys. Rev. Lett.* **64**, 3070 (1990).
- [20] J.M. Kikkawa and D.D. Awschalom, *Phys. Rev. Lett.* **80**, 4313 (1998).
- [21] F. Meier, B.P. Zakharchenya, Eds., *Optical Orientation* (North-Holland, New York, 1984) and references therein.
- [22] G. Salis *et al.*, *Phys. Rev. Lett.* **86**, 2677 (2001).
- [23] The traditional tunneling current polarization is $(|t_+|^2 - |t_-|^2)/(|t_+|^2 + |t_-|^2) = (|r_-|^2 - |r_+|^2)/(2 - |r_-|^2 - |r_+|^2)$. In the high barrier regime, this quantity can be as high as 30 % (not shown) because $|r_-|^2 \approx |r_+|^2 \approx 1$.
- [24] W. Van Roy *et al.*, *J. Cryst. Growth* **227**, 852 (2001).
- [25] M. Tanaka, K. Takahashi, *J. Cryst. Growth* **227**, 847 (2001).